Hybrid Two-Dimensional Correlation and Parallel Factor Studies on the Switching Dynamics of a Surface-Stabilized Ferroelectric Liquid Crystal

Yuqing Wu,[†,‡] Bo Yuan,[†] Jing-Gang Zhao,[†] and Yukihiro Ozaki*[,†]

Department of Chemistry, School of Science and Technology, Kwansei-Gakuin University, Gakuen, Sanda, Hyogo 669-1337, Japan, and Key Laboratory for Supramolecular Structure and Materials of Ministry of Education, Jilin University, Changchun 130023, P. R. China

Received: August 7, 2002

Sample−sample (SS) two-dimensional (2D) correlation spectroscopy has been applied to polarization-angle-dependent infrared (IR) spectra of a surface-stabilized ferroelectric liquid crystal, FLC-3, and hybrid 2D correlation spectroscopy has been applied to its time-dependent and polarization-angle-dependent IR spectra to explore the switching dynamics of the FLC. A new multiparameter analysis method, parallel factor (PARAFAC), has also been used to analyze both the time-dependent and polarization-angle-dependent IR spectra. The synchronous and asynchronous SS hybrid 2D correlation spectra generated from the time-dependent spectra and the polarization-angle-dependent spectra of FLC-3 provide information about its dynamic behavior induced by the two independent perturbations, the polarization angle and delay time. Hybrid 2D correlation cannot be used for the prediction such as that of a change in the polarization angle with the delay time. In contrast, PARAFAC can predict effects of any level of the factors investigated as well as the multiplicative interactions between the different factors. Both hybrid 2D and PARAFAC are powerful to illustrate the relationship between the spectral changes caused by the two perturbations, the polarization angle and the delay time for FLC-3. Hybrid 2D and PARAFAC can supply important information about main effects and the additive effective, lower order interactions in a spectral decomposition. In this way the new spectral analysis methods yield more precise and deeper information about the dynamics of FLC-3 efficiently.

Introduction

For the past decade, polarization infrared (IR) spectroscopy and time-resolved IR spectroscopy have been utilized extensively for investigating the static orientation and the dynamic behavior of liquid crystalline molecules.[1−20] Polarization IR spectroscopy provides information about the direction of transition dipole moments of normal modes of vibrations. Measurements of the polarization angle dependences of IR bands of a ferroelectric liquid crystal (FLC) in the Sm-*C** phase are very useful to explore its molecular structure and alignment. However, the analysis of the polarization angle dependences of IR band intensities is not always straightforward. The theoretical relationship between absorbance of an IR band and polarization angle has been studied by our group for a FLC named FLC-3.[19] We analyzed in detail the dependence of the absorbance upon the polarization angle and provided new insight into the relation between the transition moment and the molecular long axis.

Time-resolved vibrational spectroscopy, especially time-resolved IR absorption spectroscopy, is of particular usefulness for exploring orientational and conformational changes during the electric-field-induced dynamical switching of a FLC in the Sm-*C** phase.[1−16,18,20] Several time-resolved IR studies have indicated that during the electric-field-induced dynamical switching, FLC molecules reorient as rigid units, in other words, all the molecular segments reorient nearly simultaneously. On the other hand, other studies have showed that different molecular segments have different responses and reorientation times. It seems that each FLC shows different dynamic behavior. Despite intensive time-resolved IR studies on the switching dynamics of FLCs at a molecular segmental level, many basic aspects of the dynamical behavior of FLCs have not yet been clarified.

The purpose of the present study is to demonstrate the potential of two new spectral analysis methods, hybrid two-dimensional (2D) correlation spectroscopy and parallel factor (PARAFAC) in the analysis of polarized IR and time-resolved IR spectra of FLCs. The introduction of the new spectral analysis methods is very important because one may be able to analyze the spectra more precisely, deeply, and efficiently even if the spectra are rather noisy.

Hybrid 2D correlation spectroscopy, which was proposed by ourselves in 2002,[21] is a new extension of generalized 2D correlation spectroscopy.[22−24] 2D correlation spectroscopy, which consists of synchronous and asynchronous spectra, simplifies complex spectra consisting of many overlapped peaks and enhances spectral resolution by spreading peaks along the second dimension, enabling one to extract information that cannot be obtained straightforwardly from one-dimensional spectra.[22−24] Recently, there was important progress in 2D correlation spectroscopy. Šašić et al.[25] have proposed a new kind of 2D correlation spectroscopy. It is called sample−sample correlation spectroscopy. In sample−sample correlation spectroscopy, 2D correlation maps having sample axes are generated instead of creating 2D maps with variable (wavelength or wavenumber) axes.[25] In the usual 2D (variable−variable)

* To whom correspondence should be addressed. E-mail: ozaki@ksc.kwansei.ac.jp. Fax: +81-79-565-9077.

[†] Mailing address: Yukihiro Ozaki; Department of Chemistry, School of Science and Technology, Kwansei-Gakuin University, Gakuen, Sanda, Hyogo 669-1337, Japan.

[‡] Jilin University.

10.1021/jp021817c CCC: $25.00
Published on Web 07/08/2003

correlation spectroscopy, the correlations between bands are discussed, while in sample-sample correlation spectroscopy, concentration dynamics are investigated. Thus, variable−variable correlation spectroscopy and sample−sample correlation spectroscopy are totally complementary.

However, for all the 2D correlation analyses until recently, synchronous and asynchronous spectra have been constructed from a series of spectra obtained under one particular perturbation and for one particular system. There were a few questions. Is it possible to construct 2D correlation spectra between two series of spectra measured under two different kinds of perturbations such as temperature and pressure? Can we generate 2D correlation spectra from two different but related systems such as the same reaction by different catalysts? Such kinds of questions resulted in new breakthroughs in 2D correlation spectroscopy, hybrid 2D correlation spectroscopy.[21]

Hybrid 2D correlation spectroscopy has three possibilities.[21] In the first, 2D correlation spectra are calculated by using different sets of spectral data of the same sample obtained under two kinds of perturbations such as temperature and pressure. In the second, 2D correlation spectra are constructed by using spectral variations measured under conjunct or related perturbations. The third treats 2D correlation spectra generated by using two independent spectral data collected under the same perturbation but under different conditions such as the same chemical reaction with different catalysts. In all the cases hybrid 2D correlation spectroscopy allows one to discuss directly the correlation between two independent spectral data sets and therefore extract additional information such as that about the comparison of effects of two different perturbations and the comparison of two different systems.[21] By use of this method, one can explore directly the correlations between two systems or spectral data sets measured under two different perturbations. By analogy to the existing 2D correlation spectroscopy,[22−24] the hybrid 2D correlation spectroscopy has also variable−variable (VV) and sample−sample (SS)[25] correlation spectroscopy.[21]

PARAFAC is a newly developed decomposition method that can be conceptually treated as an application of bilinear principal component analysis (PCA) for multiway data.[26−28] It has been gaining more and more interest for chemometrics and related fields for its obvious advantage over PCA;[29−31] The algorithms of PARAFAC used are most often based on alternating least squares (ALS) initialized by either random values or values calculated by a direct trilinear decomposition based on the generalized eigenvalue problem. The reason for using multiway PARAFAC is not to obtain better fit but to develop more adequate, robust, and interpretable models as a multiplicative effect of several different factors.[26]

It is possible for PARAFAC to predict the effects of any level of the factors investigated as well as the multiplicative interactions between the different factors. Meanwhile, it should be emphasized that multiway data are characterized by several sets of variables that are measured in a cross fashion. In the present study, we use PARAFAC to analyze the cross data set of polarization-angle and time-resolved IR spectra of FLC-3 (Figure 1).

In this paper we report the potential of SS 2D correlation spectroscopy, hybrid 2D correlation spectroscopy, and PARAFAC in analyzing the polarization-angle-dependent and time-resolved IR spectra of FLC-3. We also compare hybrid 2D correlation and PARAFAC analyses. These novel spectral analysis methods should play very important roles in unraveling complicated

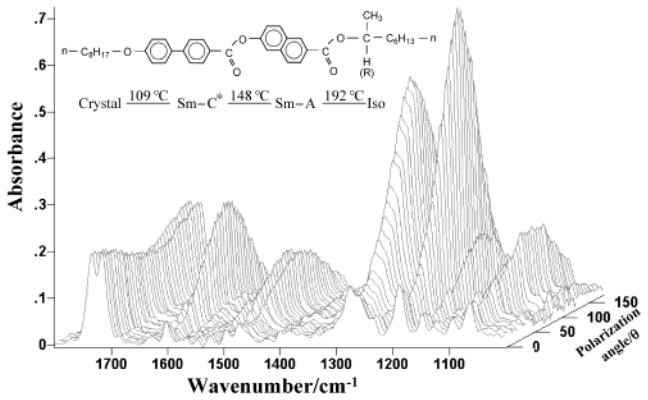

Figure 1. Structure and phase transitions of FLC-3. Time-dependent IR spectra of FLC-3 in the Sm-*C** phase at 137 °C at a rectangular electric field of ±40 V with 5-kHz repetition rate for delay times from 0.5 to 30.5 μs.

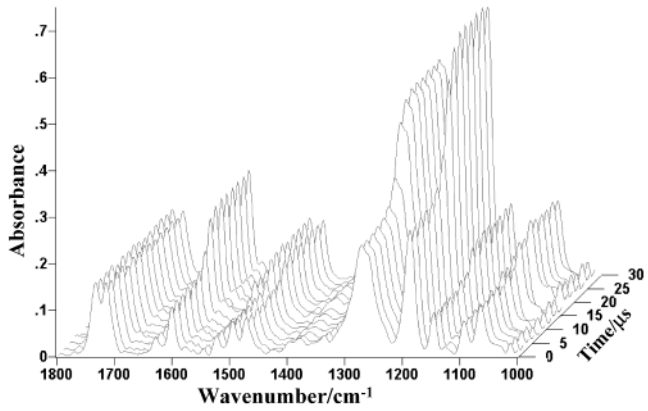

Figure 2. Polarization-angle-dependent IR of FLC-3 in the Sm-*C** phase at 137 °C at a rectangular electric field of ±40 V with a 5-kHz repetition rate for polarization angles from 0° to 180° with intervals of 5°.

spectra measured under perturbation and comparing the spectra obtained under different perturbations.

Experimental Section

The preparation of sample and the IR measurements were the same as those reported in the previous papers.[19,20]

Software for the sample−sample 2D and hybrid 2D correlation analyses was composed by one of the authors (Y. Wu) based on Metlab 6.0 (MathWorks Inc., Natic, MA).[21] The software of PARAFAC was downloaded from http://newton.foodsci.kvl.dk\foodtech.html.[26]

Results and Discussion

1. Polarization-Angle Dependent and Time-Resolved IR Spectra. Figure 1 shows polarization-angle-dependent IR spectra in the region of 3200−1200 cm^{-1} of FLC-3 in the Sm-*C** phase at 137 °C at a rectangular electric field of ±40 V with 5-kHz repetition rate for the delay time of 0.5 μs. Figure 2 exhibits time-resolved IR spectra of FLC-3 in the Sm-*C** phase at 137 °C at a rectangular electric field of ±40 V with 5-kHz repetition rate at the polarization angle of 60°. The band assignments of the IR spectra of FLC-3 were reported in our previous papers.[19,20]

2. SS 2D Correlation Analysis of Polarization Angle-Dependent IR Spectra. Figure 3 displays the slice spectra extracted from (A) synchronous and (B) asynchronous SS 2D correlation spectroscopy constructed from the polarization-angle-dependent IR spectra from 0° to 180° at an interval of 5° in the 1220−1165 cm^{-1} region of FLC-3 in the Sm-*C** phase at 137

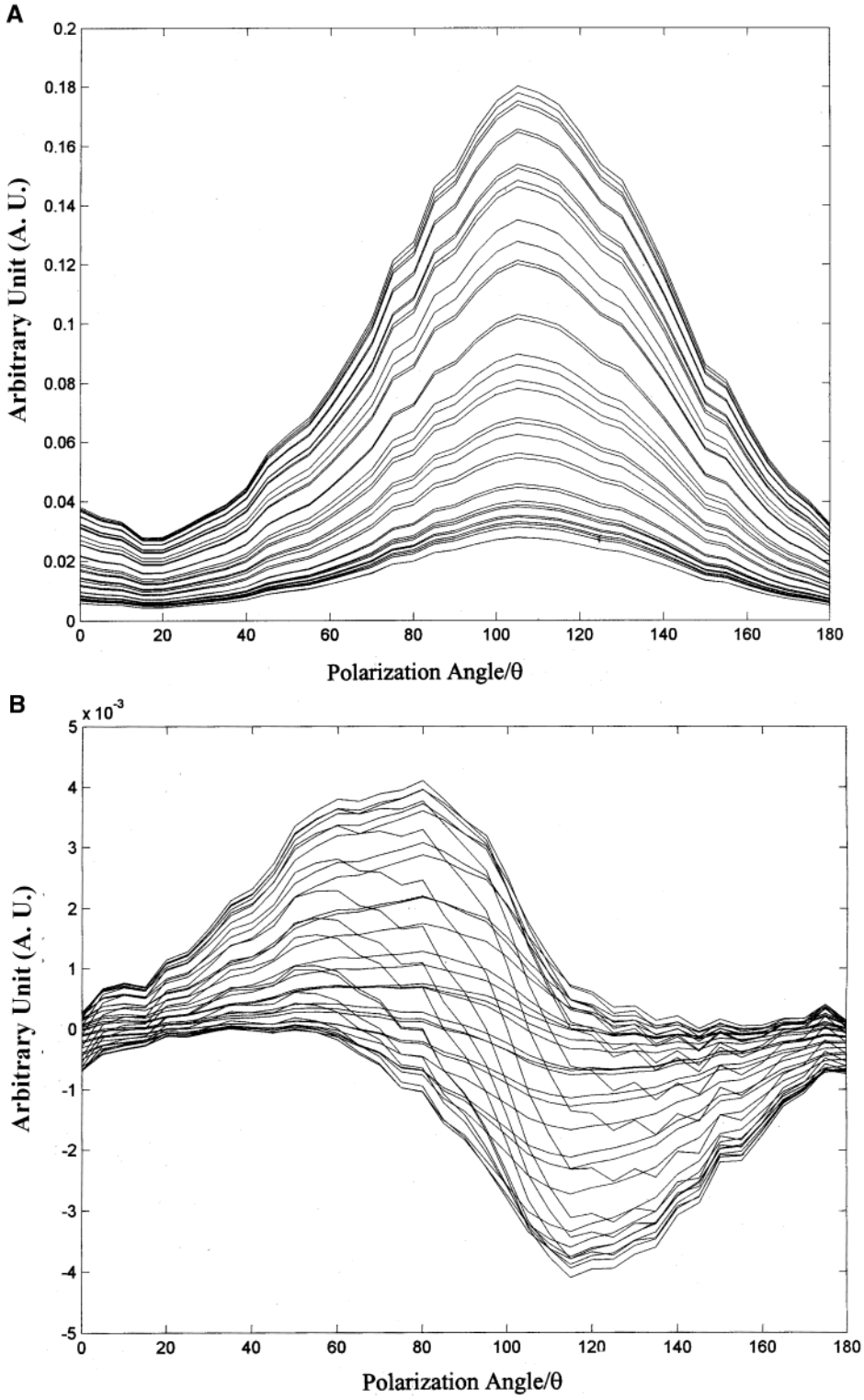

Figure 3. Slice spectra obtained from (A) synchronous and (B) asynchronous SS 2D correlation maps constructed from the polarization-angle-dependent IR spectra in the 1220−1165 cm^{-1} region of FLC-3 in the Sm-*C** phase at 137 °C at a rectangular electric field of ±40 V with 5-kHz repetition rate for the delay time of 0.5 μs.

°C at a rectangular electric field of ±40 V with 5-kHz repetition rate for the delay time of 0.5 μs. A significant peak is observed at the polarization angle of 103° in the synchronous slice spectra (Figure 3A). This means that the average of maximum band intensity is located at the polarization angle of 103°, which illustrates the orientation projection direction of the molecular long axis in the cell window. The plots in Figure 3A are very similar to the plots of the normalized absorbance versus the polarization angle reported in our previous study.[19] This means that the synchronous slice spectra in Figure 3A reveal nothing more than the microscopic mechanism of the electric-field-induced reorientation of the C−O−C group revealed by the relationship between the absorbance of the band at 1188 cm^{-1} versus the polarization angle.

Of interest is that the asynchronous slice spectra in Figure 3B have high similarity to the plots of $\Delta A(t)$ and $\Delta A(0.5)$ versus the polarization angle for the band at 1602 cm^{-1} (under identical physical conditions; in the Sm-C* phase at 137 °C at a

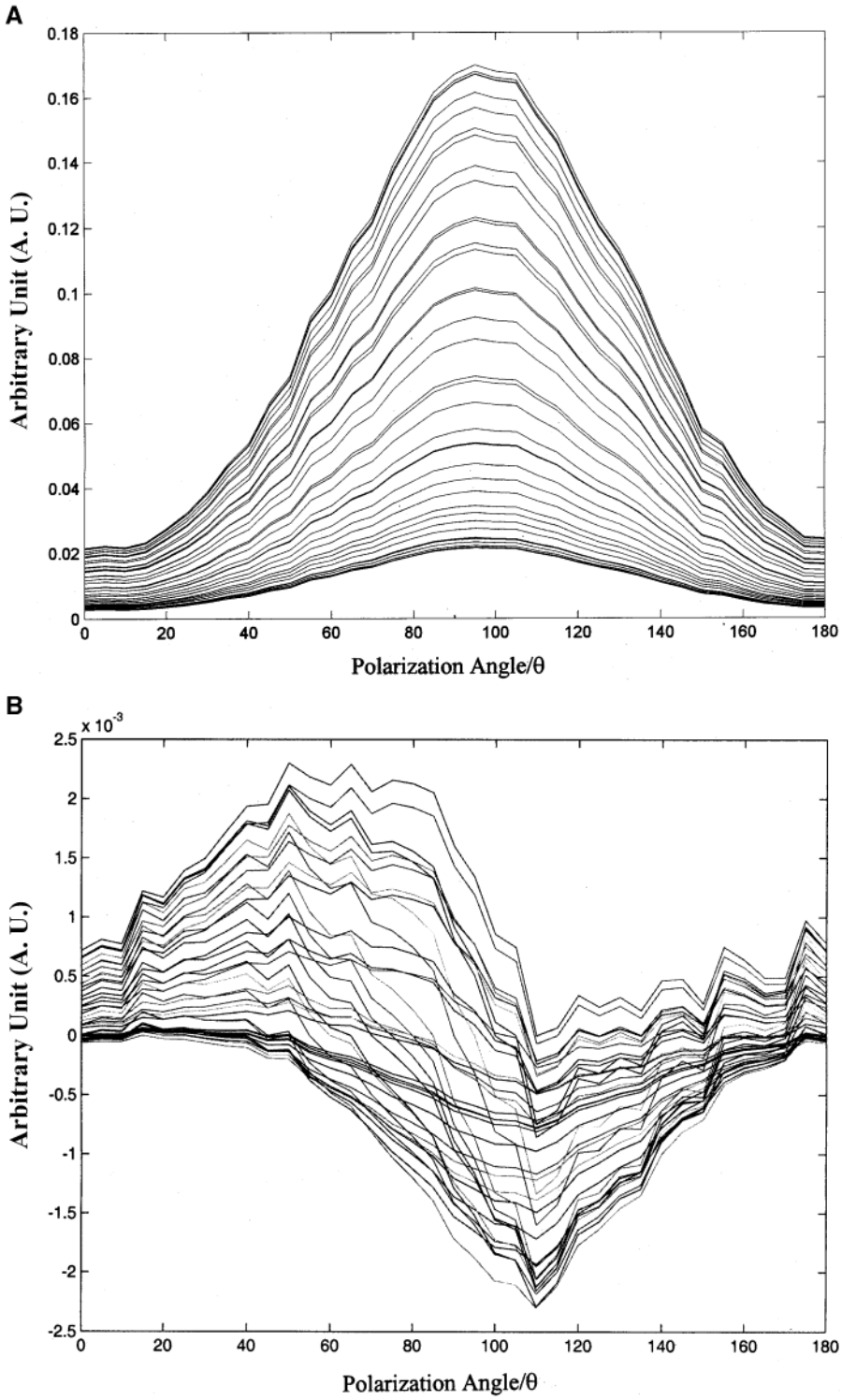

Figure 4. Slice spectra obtained from (A) synchronous and (B) asynchronous SS 2D correlation maps constructed from the polarization-angle-dependent IR spectra in the 1220−1165 cm^{-1} region of FLC-3 in the Sm-C* phase at 137 °C at a rectangular electric field of ±40 V with 5-kHz repetition rate for the delay time of 12.5 μs.

rectangular electric field of ±40 V with 5-kHz repetition rate.).[20] Here, $\Delta A(t)$ and $\Delta A(0.5)$ correspond to the difference absorbance between the current and the last delay time [$\Delta A(t)$] and the delay time of 0.5 μs [$\Delta A(0.5)$], respectively, for delay times of 2.5, 4.5, ...28.5, 30.5 μs.[20] A synchronous spectrum represents simultaneous spectral changes at any pair of spectral coordinates, while an asynchronous spectrum represents sequential or unsynchronized variations, and asynchronicity is essentially connected with the nonproportionality in the spectral variations.[22,23] Therefore, it seems quite reasonable to obtain similar results by using the conventional method and SS 2D correlation analysis. It is not always easy to grasp clear physical meaning of an asynchronous SS correlation spectrum. However, in the present study, the SS asynchronous spectra are related to clear physical meaning; polarization-angle-dependent microscopic mechanism of FLC-3.

To explore the time-dependent behavior of FLC-3 at different polarization angles in more detail, SS 2D correlation spectra were constructed for every delay time between 0.5 and 30.5 μs. Comparison of the SS 2D correlation slice spectra obtained

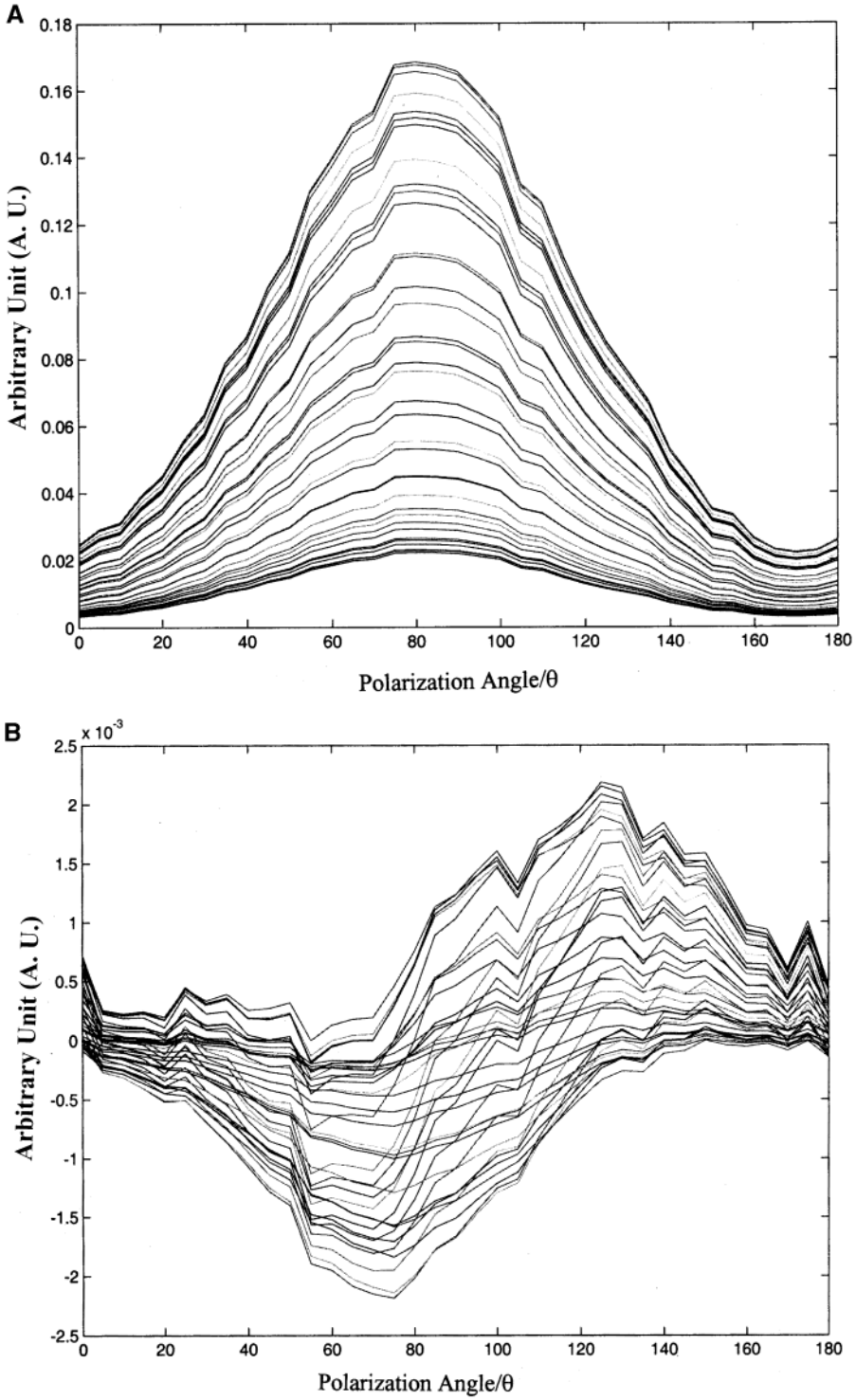

Figure 5. Slice spectra obtained from (A) synchronous and (B) asynchronous SS 2D correlation maps constructed from the polarization-angle-dependent IR spectra in the 1220−1165 cm^{-1} region of FLC-3 in the Sm-*C** phase at 137 °C at a rectangular electric field of ±40 V with 5-kHz repetition rate for the delay time of 14.5 μs.

reveals that the polarization angle for the maximum absorbance is kept constant for delay times from 0.5 to 10.5 μs. However, significant changes are observed between delay times of 12.5 and 14.5 μs. Figures 4 and 5 illustrate slice spectra obtained from (A) synchronous and (B) asynchronous SS 2D correlation spectroscopy constructed from the polarization-angle-dependent IR spectra in the 1220−1165 cm^{-1} region of FLC-3 for the delay times of 12.5 and 14.5 μs, respectively. The maximum absorbance is observed at the polarization angle of 94° and 80° for the delay time of 12.5 and 14.5 μs, respectively. These two angles are far from the angle showing the maximum absorbance at other delay times. This means that the orientation of the FLC molecules at delay times of 12.5 and 14.5 μs makes a larger inclination than that at other delay times with respect to the plane of the cell window. These experimental results suggest that the FLC molecules rotate on the orbit of the cone.

The previous study showed that the polarization angles of 97.21 and 80.91° give the maximum absorbance for the delay

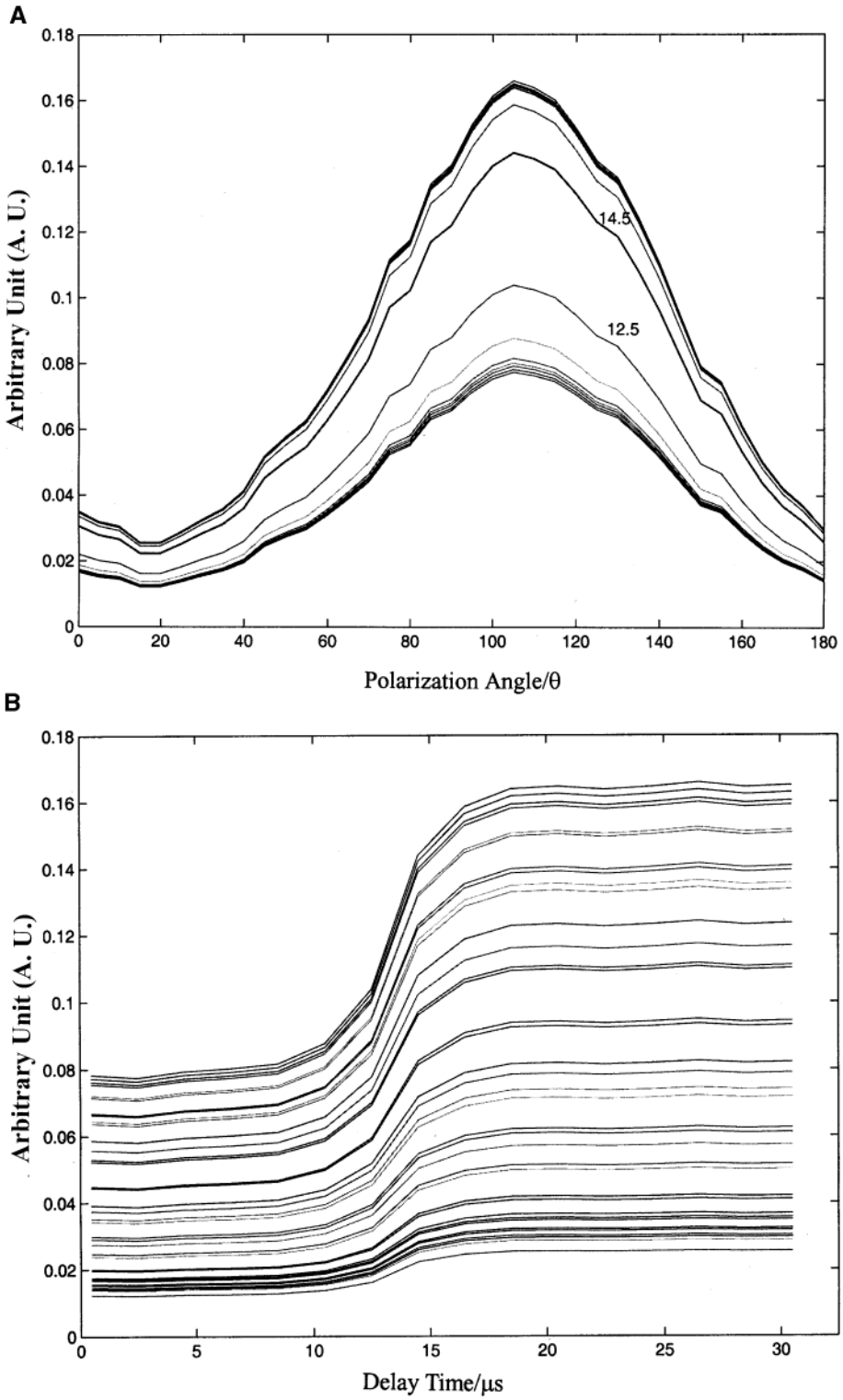

Figure 6. Synchronous slice spectra extracted from the axes of (A) delay time and (B) polarization angle.

time of 12.5 and 14.5 μs, respectively.[20] The present results are in a good agreement with those obtained in the previous study.

Comparison of the slice spectra in Figures 3B and 4B reveals that the polarization angles corresponding to the maximum or minimum absorbance shift to smaller values with the increase in the delay time from 0.5 to 12.5 μs. This is in good agreement with the previous investigation, which demonstrated that at each delay time, the curves of both $\Delta A(t)$ and $\Delta A(t_{0.5})$ have the maximum and minimum absorbance versus a certain polarization angle and that the polarization angles shift to smaller values with the increase in delay time.[20] The decrease in the polarization angles giving the maximum and minimum absorbance may be ascribed to the switching motion of the FLC molecules on the tilt cone. While the comparison between Figures 4B and 5B shows opposite change sequences between the delay times of 12.5 and 14.5 μs, the results in both figures manifest that significant changes in the molecular orientation occur between the delay time of 12.5 and 14.5 μs. The differentiations revealed by the polarization-angle-dependent SS 2D correlation illustrate

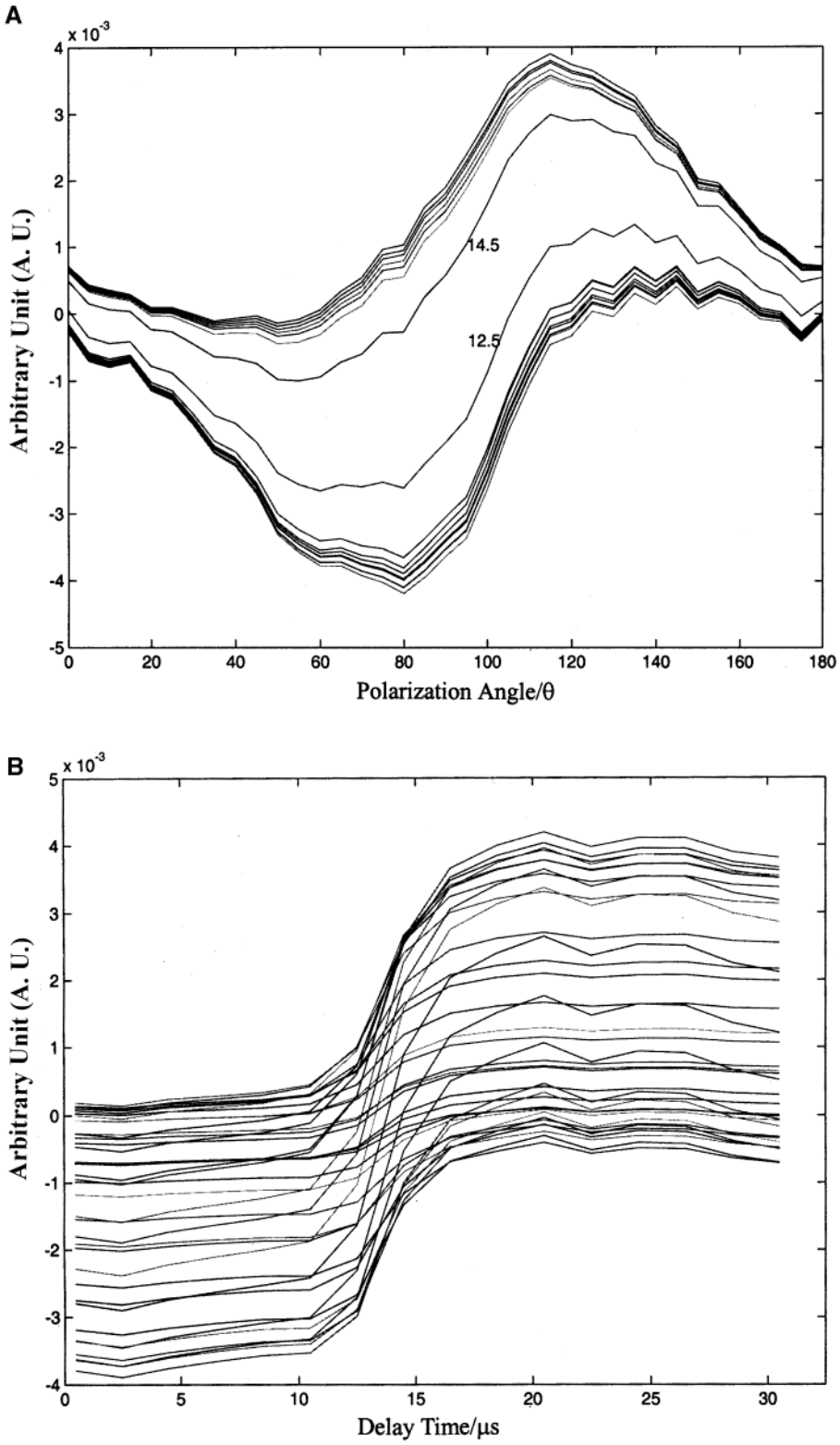

Figure 7. Asynchronous slice spectra extracted from the axes of (A) delay time and (B) polarization angle.

that in order to analyze precisely the reorientation of the segments as a function of the delay time, it is very important to select an appropriate polarization angle.

3. Hybrid 2D Correlation Spectra Constructed from Polarization-Angle-Dependent IR Spectra and Time-Resolved IR Spectra. The changes in the direction of the molecular long axis of FLC-3 with the delay time were demonstrated by using a few representative IR bands,[20] and the mechanism of changing the direction was investigated also by SS 2D correlation analysis of the time-resolved IR data.[32]

The synchronous and asynchronous SS hybrid 2D correlation spectra were constructed from the time-dependent IR spectra of FLC-3 in the Sm-*C** phase at 137 °C at a rectangular electric field of ±40 V with 5-kHz repetition rate at the polarization angle of 60° and the polarization-angle-dependent IR spectra at 137 °C at a rectangular electric field of ±40 V with 5-kHz

repetition rate at the delay time of 0.5 μs. The synchronous slice spectra extracted from the axes of delay time and polarization angle are demonstrated in parts A and B of Figure 6, respectively. The corresponding asynchronous ones are shown in part A and B of Figure 7, respectively. The synchronous slice spectra along the axis of the polarization angle indicate that a polarization angle of 103° gives the maximum absorbance. This result is exactly the same as that revealed by the polarization-angle-dependent SS 2D correlation spectra in Figure 3A. Moreover, a significant jump is observed between the delayed times of 12.5 and 14.5 μs (Figure 6), which cannot be achieved by the normal SS 2D correlation analysis. That is, hybrid 2D can supply important information about the dynamics of FLC-3 induced by the two independent perturbations at the same time, for example, polarization angle and delay time, in the present study. The slice spectra in Figure 6B along the axis of delay time confirm the above conclusion.

The hybrid 2D asynchronous slice spectra in Figure 7 provide information about the sequential or unsynchronized variations. Note that strong positive and negative correlations are observed at 83° and 117° in Figure 7A, respectively. The big jump is also observed both in the slice spectra of Figure 7, which corresponds to the changes for the delay time from 12.5 to 14.5 μs.

Hybrid 2D correlation can supply useful information about the correlations between two separated variables directly.[21] Thus, we expected to extract information about the change in the polarization angle with the delay time, for example, the change from 103° to 80° during the time course from 0.5 to 14.5 μs. However, we could not extract such information. Therefore, we concluded that hybrid 2D correlation cannot be used for the predication because it originates from only a two-way matrix at the fixed variables. In this sense, PARAFAC may supply more information than hybrid 2D because it is constructed from a multiway matrix with cross variables.[26−28]

4. PARAFAC Analysis of IR Spectra of FLC-3. For exploring the influence of the polarization angle and the delay time on the structure and orientation of FLC-3 in the Sm-*C** phase and the relationship between these two variables, a multiway analysis method, PARAFAC, is applied in the present study. Building a calibration model to predict the ideal experimental conditions would suggest how the structure and orientation of FLC-3 are affected by the different factors.

In the PARAFAC model, three different modes (ways) are polarization-angle (dimension 37), delay time (dimension 16), and wavenumber (dimension 19). The *ijk*th element of the three-way array contains the influence of the *i*th level of wavenumber, the *k*th level of the polarization angle, and the *j*th level of delay time. The whole array is seen as the number of samples of 16 × 37 × 19, and the data are interpreted as a three-way array.

A one-component solution was performed based on the three-way array above. From the PARAFAC loadings it is possible to predict an effect at any level of factors investigated. The loading vectors of the one-component model are shown in Figure 8. The unconstrained one-component PARAFAC explains only 93.4889 of the explained variations and with a very high sum-of-squares of residuals of 41.493. This means that the principal component and/or the constraints do not perform perfectly. Even so, it is still possible to predict the effect of the three factors investigated by the loading vector plots of the three models in Figure 8.

One of the characteristics of the three-way method different from an ordinary two-way case is that there is no rotation problem in PARAFAC; e.g., pure spectra can be recovered from

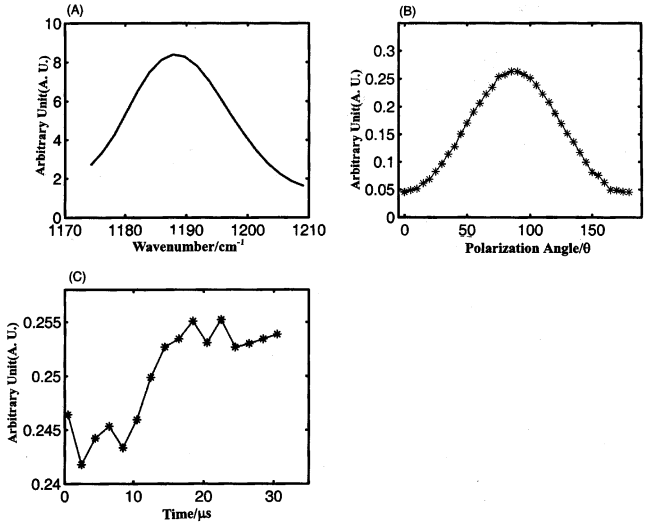

Figure 8. Loading vectors of one-component PARAFAC model constructed from IR spectra of FLC-3.

multiway spectral data.[26−28] The loading plot of the first model in Figure 8A proves the above character clearly, which represents nothing more than the extracted pure spectrum of the band centered at 1188 cm^{-1}. It gives the general distribution of the band intensity along the wavenumber axis.

However, the loading plot in Figure 8B represents much more physical meaning than that in Figure 8A. It reveals the relationship between the band intensity at 1188 cm^{-1} and the polarization angle. The polarization angle giving the maximum absorbance is observed around 86°, which is lower than 103° at the delay time of 0.5 μs and higher than 80° at the delay time of 14.5 μs as revealed by the polarization-angle-dependent SS 2D correlation analysis described above. The result in Figure 8B is quite reasonable, and the loading vectors revealed by the three-way PARAFAC method represent mean features of the IR spectra within the whole range of delay time (from 0.5 to 30.5 μs). It cannot be identical with any result obtained by SS 2D correlation analysis at a certain delay time. In this sense, the SS hybrid 2D correlation has unsurpassed merit in comparison with the PARAFAC analysis.

The switching dynamics of the surface-stabilized ferroelectric liquid crystal, FLC-3, is revealed by the loadings vectors plot of Figure 8C. It represents the time-dependent orientation change of the C−O−C group by the selected band at 1188 cm^{-1} during the course of electric-field-induced switching. This orientation change may be caused by the revolution of the molecule around its own axis induced by the electric torque $\Gamma = PE$, where P is the total polarization of FLC-3.[33]

It is noted that the relationship between the band intensity and the delay time shown in Figure 8C does not fit very well with that achieved by the SS hybrid 2D correlation (Figures 6 and 7). A significant change is observed between the delay times of 10.5 and 12.5 μs in Figure 8C. On the other hand, a major change is observed between the delay time of 12.5 and 14.5 μs in the SS 2D correlation slices in Figures 6 and 7. Moreover, the loadings plot shown in Figure 8C is somewhat noisy in comparison with the other two models in Figure 8A,B. The comparison between the loadings plots of one-component PARAFAC and the slice spectra of SS 2D (Figures 3−5) and/or hybrid SS 2D (Figures 6 and 7) spectra reveal that one-component may not be enough for the present three models, especially for the model three.

In an effort to develop a better model and to improve the quality of the validation, we have improved the number of the

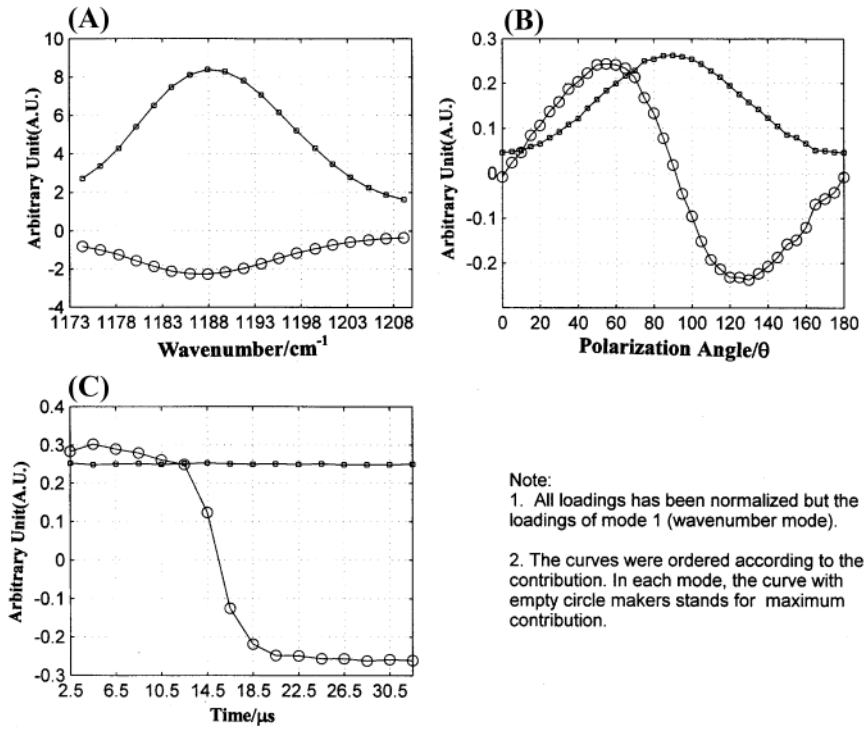

Figure 9. Loading vectors of the two-component PARAFAC model without constraint constructed from IR spectra of FLC-3.

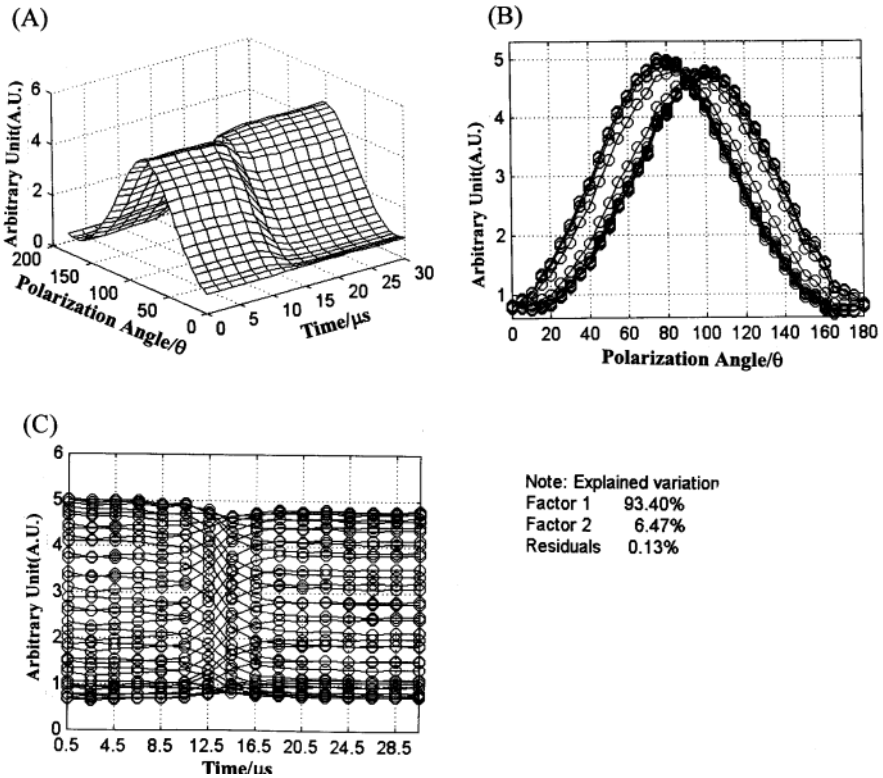

Figure 10. (A) Multiplying the loading vectors of the second model by that of the third model. Slice spectra along the axis of (B) the polarization-angle and (C) the delay time.

iterations. Figure 9 illustrates the loadings vectors from two-iteration PARAFAC model. The sum-of-squares of residuals and explained variation for the unconstrained two-component PARAFAC have been improved significantly to 0.8391 and 99.868, respectively. As we have estimated, for the first mode, the second component does not show much more interesting result than the first one.

Of interest is the loading plot in Figure 9B. One can clearly observe reasonable shape in the loadings vectors of the first two components; the first one is very similar to the slice spectra of the synchronous spectrum constructed from the polarization-angle-dependent SS 2D correlation analysis (see Figures 3A, 4A, and 5A), while the second loading is very similar to the slice spectra of the corresponding asynchronous spectrum (see

Figures 3B, 4B, and 5B). This conclusion is analogous to the comparison of the loading plots of PCA constructed from concentration-dependent near-infrared spectral variations of human serum albumin with their VV 2D correlation slice spectra reported by Murayama et al.[34] It implies the high consistency between two-way PCA and three-way PARAFAC analysis. Of course, PARAFAC has its own specification compared with two-way PCA as we have mentioned above. More discussion of the specification will be addressed later.

The loading vector for the second component in Figure 9C shows the opposite trend. However, it is quite consistent with the results of time-dependent SS hybrid 2D correlation. Significant changes are observed at the delay time of 12.5 and 14.5 μs, illustrating the power of PARAFAC in revealing the mechanism of the physical process.

Different constrained methods, for example, orthogonal, nonnegative, and unimodal models, have been tried to improve the results separately. The results have shown that no significant improvement is achieved by these constrained methods. For example, by using the nonnegative constraint, the sum-of-squares of residuals and explained variation for the unconstrained one-component PARAFAC are kept almost the same as the nonconstrained two-components analysis. Therefore, we do not show the loading plots of constrained two components here.

5. Comparison of Hybrid SS 2D Correlation Spectroscopy and PARAFAC Analysis. To illustrate the relationship between the polarization angle and the delay time for FLC-3, multiplying the loading vectors of the second model by that of the third model was performed. Figure 10A shows the result. The slice spectra extracted along the axis of the polarization angle and the delay time are shown in parts A and B of Figure 10, respectively. Of note is that both the changes in the polarization angle corresponding to the maximum and/or minimum absorbance at each delay time (Figure 10B) and the significant time-dependent changes in the delay time between 12.5 and 14.5 μs (Figure 10C) are observed simultaneously in Figure 10. In this sense, PARAFAC demonstrates more powerful illustration in comparison with hybrid 2D correlation spectroscopy.

Conclusion

The present study has demonstrated that both hybrid 2D correlation spectroscopy and PARAFAC are very powerful in analyzing the polarization-angle-dependent and time-resolved IR spectra of FLC-3. The following conclusions can be drawn from the present study: (1) Both hybrid 2D correlation spectroscopy and PARAFAC can be applied to the multiway array data to extract more unambiguous information than those obtained by normal 2D correlation analysis and two-way PCA. (2) Both can supply important information about the main effect and additive effective, lower order interactions in spectral decomposition. Moreover, the main effect and lower order interactions can be distinguished clearly. Meanwhile, it should be emphasized that multiway data are characterized by several sets of variables that are measured in a cross fashion. Therefore, from the PARAFAC loadings, it is possible to predict the effect of any level of the factors investigated as well as the multiplicative interaction between the different factors. In contrast, hybrid-2D correlation cannot be used for the prediction because it originated from only a two-way matrix at the fixed variables. On the other hand, the SS hybrid-2D correlation analysis has an advantage over the PARAFAC method in that the loading vectors revealed by the three-way PARAFAC method represent only mean features of the IR spectra.

Acknowledgment. The present study was supported by a Grant-in-Aid to Y. Ozaki (11695033) from the Ministry of Education, Science, and Culture, Japan.

References and Notes

(1) Kocot, A.; Vij, J. K.; Perova, T. S. In Advances in Liquid Crystals. *Advanced in Chemical Physics*; Vij, J. K., Ed.; Wiley: New York, 2000; Vol. 113, p 103.
(2) Shilov, S. V.; Okretic, S.; Siesler, H. W. *Vib. Spectrosc.* **1995**, *9*, 57.
(3) Czarnecki, M. A.; Katayama, N.; Ozaki, Y.; Satoh, M.; Yoshio, K.; Watanabe, T.; Yanagi, T. *Appl. Spectrosc.* **1993**, *47*, 1382.
(4) Urano, T.; Hamaguchi, H. *Appl. Spectrosc.* **1993**, *47*, 2108.
(5) Gregoriou, V. G.; Chao, J. L.; Toriumi, H.; Palmer, R. A. *Chem. Phys. Lett.* **1991**, *179*, 491.
(6) Czarnecki, M. A.; Katayama, N.; Satoh, M.; Watanabe, T.; Ozaki, Y. *J. Phys. Chem.* **1995**, *99*, 14101.
(7) Katayama, N.; Sato, T.; Ozaki, Y.; Murashiro, K.; Kikuchi, M.; Saito, S.; Demus, D.; Yuzawa, T.; Hamaguchi, H. *Appl. Spectrosc.* **1995**, *49*, 977.
(8) Shilov, S. V.; Okretic, S.; Siesler, H. W.; Zentel, R.; Oge, T. *Macromol. Rapid Commun.* **1995**, *16*, 125.
(9) Czarnecki, M. A.; Okretic, S.; Siesler, H. W. *J. Phys. Chem. B* **1997**, *101*, 374.
(10) Hide, F.; Clark, N. A.; Nito, K.; Yasuda, A.; Walba, D. M. *Phys. Rev. Lett.* **1995**, *75*, 2344.
(11) Shilov, S. V.; Okretic, S.; Siesler, H. W.; Czarnecki, M. A. *Appl. Spectrosc. Rev.* **1996**, *31*, 82.
(12) Kim, K. H.; Ishikawa, K.; Takezoe, H.; Fukuda, A. *Phys. Rev. E* **1995**, *51*, 2166.
(13) Jin, B.; Ling, Z.; Takanishi, Y.; Ishikawa, K.; Takezoe, H.; Fukuda, A.; Kakimoto, M.; Kitazume, T. *Phys. Rev. E* **1996**, *53*, R4295.
(14) Kim, K. H.; Miyachi, K.; Ishikawa, K.; Takezoe, H.; Fukuda, A. *Jpn. J. Appl. Phys. Part* 1 **1994**, *33*, 5850.
(15) Verma, A. L.; Zhao, B.; Jiang, S. M.; Shen, J. C.; Ozaki, Y. *Phys. Rev. E* **1997**, *56*, 3053.
(16) Verma, A. L.; Zhao, B.; Terauchi, H.; Ozaki, Y. *Phys. Rev. E* **1999**, *59*, 1868.
(17) Nagasaki, Y.; Yoshihara, T.; Ozaki. Y. *J. Phys. Chem. B* **2000**, *104*, 2846.
(18) Nagasaki, Y.; Masutani, K.; Yoshihara T.; Ozaki, Y. *J. Phys. Chem. B.* **2000**, *104*, 7881.
(19) Zhao, J. G.; Yoshihara, T.; Siesler, H. W.; Ozaki Y. *Phys. Rev. E* **2001**, *64*, 031704.
(20) Zhao, J. G.; Yoshihara, T.; Siesler, H. W.; Ozaki Y. *Phys. Rev. E* **2002**, *65*, 021710.
(21) Wu, Y.; Jiang, J.-H.; Ozaki, Y. *J. Phys. Chem. A.* **2002**, *16*, 2422.
(22) Noda, I. *Appl. Spectrosc.* **1993**, *47*, 1329.
(23) Noda, I.; Dowrey, A. E.; Marcott, C.; Story, G. M.; Ozaki, Y. *Appl. Spectrosc.* **2000**, *54*, 236A.
(24) Ozaki, Y., Noda, I., Eds. *Two-Dimensional Correlation Spectroscopy*; American Institute of Physics: New York, 2000.
(25) Šašic, S.; Muszynski, A.; Ozaki, Y. *J. Phys. Chem. A* **2000**, *104*, 6380.
(26) Rasmus, B. *Chemom. Intel. Lab. Syst.* **1997**, *38*, 149.
(27) Claus, A. A.; Rasmus, B. *Chemom. Intel. Lab. Syst.* **2000**, *52*, 1.
(28) Juan, A.; Tauler R. *J. Chemom.* **2001**, *15*, 749.
(29) Scarminio, I.; Kubista, M. *Anal. Chem.* **1993**, *65*, 409.
(30) Sarabia, L.; Oritz, M. C.; Leardi, R.; Drava, G. *Trends Anal. Chem.* **1993**, *12*, 226.
(31) Faber, N. M.; Buydens, M. C.; Kateman, G. *J. Chemom.* **1994**, *8*, 147.
(32) Zhao, J. G.; Jiang, J.-H.; Yoshihara, T.; Siesler, H. W.; Ozaki Y. *J. Phys. Chem. B*, submitted for publication.
(33) Lagerwall, S. T. *Ferroelectric and Antiferroelectric Liquid Crystal*; Wiley-VCH: Weinheim, 1999; p 170.
(34) Murayama, K.; Czarnik-Matusewicz, B.; Wu, Y.; Tsenkova, Y.; Ozaki, Y. *Appl. Spectrosc.* **2000**, *54*, 978.